



pH-promoted *O*- α -glucosylation of flavonoids using an engineered α -glucosidase mutant

Chao Li^{a,1,2}, Jetendra Kumar Roy^{a,2}, Ki-Cheul Park^b, Art E. Cho^b, Jaeick Lee^a, Young-Wan Kim^{a,*}

^a Department of Food and Biotechnology, Korea University, 2511 Sejong-Ro, Sejong 30019, Republic of Korea

^b Department of Biotechnology and Bioinformatics, Korea University, 2511 Sejong-Ro, Sejong 30019, Republic of Korea

ARTICLE INFO

Keywords:

Retaining glycosidase
O-glycosylase
Flavonoids
pH promoted *O*- α -glucosylation

ABSTRACT

Retaining glycosidase mutants lacking its general acid/base catalytic residue are originally termed thio-glycosylases which synthesize thio-linked disaccharides using sugar acceptor bearing a nucleophilic thiol group. A few thio-glycosylases derived from retaining α -glucosidases have been classified into a new class of catalysts, O-glycosylases which transfer sugar moiety to a hydroxy group of sugar acceptors, resulting in the formation of O-linked glycosides or oligosaccharides. In this study, an efficient *O*- α -glucosylation of flavonoids was developed using an *O*- α -glycosylase derived from a thermostable α -glucosidase from *Sulfolobus solfataricus* (MaLA-D416A). The *O*-glycosylase exhibited efficient transglycosylation activity with a broad substrate spectrum for all kinds of tested flavonoids including flavone, flavonol, flavanone, flavanonol, flavanol and isoflavone classes in yields of higher than 90%. The glucosylation by MaLA-D416A preferred alkaline conditions, suggesting that pH-promoted deprotonation of hydroxyl groups of the flavonoids would accelerate turnover of covalent enzyme intermediate via transglucosylation. More importantly, the glucosylation of flavonoids by MaLA-D416A was exclusively regioselective, resulting in the synthesis of flavonoid 7-*O*- α -glucosides as the sole product. Kinetic analysis and molecular dynamics simulations provided insights into the acceptor specificity and the regioselectivity of *O*- α -glucosylation by MaLA-D416A. This pH promoted transglycosylation using *O*- α -glycosylases may prove to be a general synthesis route to flavonoid *O*- α -glucosides.

1. Introduction

Flavonoids are widely distributed polyphenols in plants and valuable secondary metabolites with significant roles for human health [1–3]. Importantly, flavonoids are naturally conjugated with carbohydrate moieties, leading to significantly enhanced stability and solubility [4]. In addition, the sugar structures predominantly affect the bio-availabilities and the adsorption in the human body [5,6]. For the adsorption in the small intestine, it is essentially requested the deglycosylation of the dietary flavonoid glycosides [6–9]. However, naturally occurring flavonoid glycosides are mostly β -glucosides which are resistant to hydrolysis of human pancreatic digestive enzymes. Although the dietary flavonoid glycosides are hydrolyzed by lactase phlorizin hydrolase in the small intestine [7,8], dietary flavonoids are not only glucosides but also in the form of various glycosides, such as

galactosides, rhamnosides, arabinosides, and rutosides [10]. Therefore, if we can simplify the sugar moiety to just glucose and invert the stereochemistry of glycosidic bonds in flavonoid glycosides from β to α -glucosidic linkage, the flavonoid *O*- α -glucosides may have improved bioavailability due to facile deglycosylation by intestinal digestive hydrolases.

Several successful attempts for α -glucosylation of flavonoids and their glycosides with sucrose using wild type transglucosidases and phosphorylases have been reported [11–15]. Recently, engineered enzymes which use sucrose as a donor sugar have been developed to improve the yields or to expand the sugar acceptor repertoires [16], however, it is still challenging due to low yields of the desired product by rehydrolysis of the products, uncontrollable sugar oligomerization and poor regioselective glycosylation. Alternatively, it would be useful to use engineered glycosidases, termed glycosynthases (Fig. 1A), which are

* Corresponding author.

E-mail address: ywankim@korea.ac.kr (Y.-W. Kim).

¹ Current address: Department of Chemistry and Biochemistry, University of Maryland, College Park, Maryland 20742, United States.

² C. L. and J. K. R. contributed equally to this work.

<https://doi.org/10.1016/j.bioorg.2020.104581>

Received 19 September 2020; Received in revised form 17 December 2020; Accepted 19 December 2020

Available online 28 December 2020

0045-2068/© 2020 Elsevier Inc. All rights reserved.

catalytic nucleophile-deficient retaining glycosidase mutants, catalysing transglycosylation using glycosyl fluorides or azides with the opposite stereochemistry to the original substrate as sugar donors [17–19]. Unfortunately, a few successful cases for the glycosynthase-based synthesis of β -glycosyl flavonoids have been reported [20,21], but no report for α -glycosyl flavonoid synthesis. By contrast, thioglycoligases (Fig. 1B) that are another class of engineered retaining glycosidase mutants generated by the mutation at its general acid/base catalytic residue are promising. Originally, thioglycoligases catalyse the synthesis of *S*-linked glycosides using thio-sugar acceptors bearing a more nucleophilic thiol group than a hydroxyl group without the assistance of the general base

catalytic residue [22–24]. Interestingly, there are a few reports regarding transglycosylation activity of the acid/base mutants toward OH groups of normal sugars, which have been termed *O*-glycoligases (Fig. 1C) [22,25,26]. Given the yields of the *O*-linked transfer products, the *O*-glycoligase activities of α -thioglycoligases are much higher than β -thioglycoligases derived from retaining α -glycosidases and β -glycosidases, respectively. The reason for the potent *O*-glycoligase activity of the α -thioglycoligases is not entirely clear, but the reactive skew boat conformation of the accumulated β -glycosyl intermediate of the acid/base α -glycosidase mutants would be helpful for the coupling with OH groups to occur [25]. Recently, the applications of *O*-glycoligases

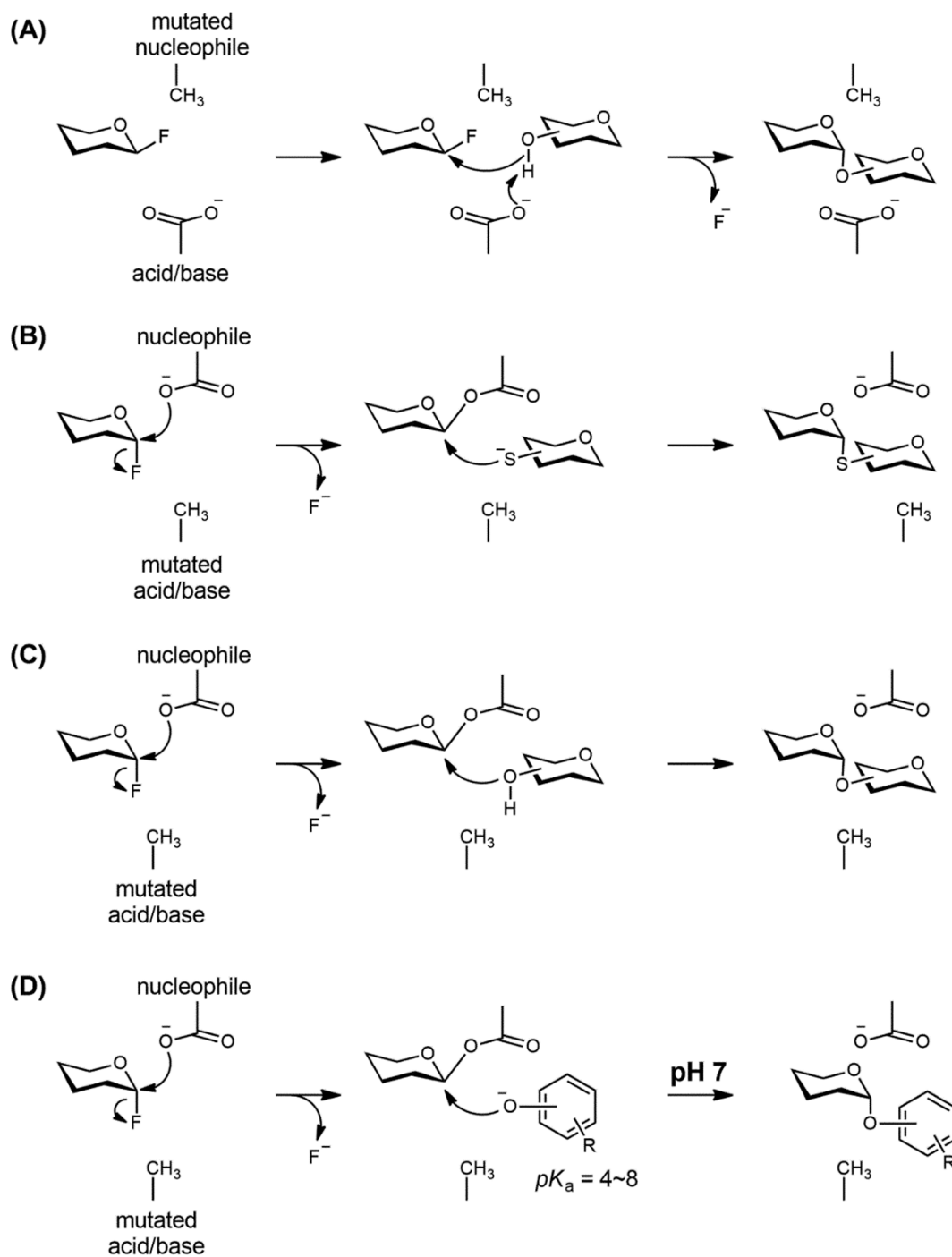


Fig. 1. Mechanism of (A) transglycosylation by α -glycosynthases toward a hydroxyl group of normal sugars; (B) transglycosylation by α -thioglycoligases toward a thiol group of synthetic thio-sugars; (C) transglycosylation by *O*-glycoligases toward a hydroxyl group of normal sugars; (D) transglycosylation by *O*-glycoligases toward a hydroxyl group of phenolic compounds with a pKa lower than that of normal sugars.

have been expanded to synthesis of *O*- α -glycosides through transglycosylation toward the hydroxyl group of simple nitrophenols and ascorbic acid containing OH groups with a pK_a value less than those of OH groups of normal sugars (Fig. 1D) [27,28].

These results raise a question as to whether *O*- α -glycosylases have potential catalytic power for direct *O*- α -glycosylation of natural flavonoid aglycones. As flavonoids are weak acids due to presence of phenolic groups, their water solubility is enhanced in alkaline pH, and naturally at high temperature [29]. In addition, reaction at an alkaline pH would promote the deprotonation of one of hydroxyl group where the glucose moiety will be transferred (Fig. 2). Here, we investigated transglycosylation by an *O*- α -glycosylase derived from a thermostable α -glucosidase from *Sulfolobus solfataricus* (MalA-D416A) [24] using various flavonoids as the substrate for α -glucosylated flavonoid synthesis.

2. Results and discussion

2.1. MalA-D416A-catalyzed transglycosylation for flavonoids

First, glycosylation of quercetin **2a** (belonging to the flavonol class) was carried out using **1** as the sugar donor. DMSO, which is commonly used as co-solvent in enzymatic reaction, was added (30% [v/v]) to increase the solubility of flavonoids in an aqueous buffer. The reaction was carried out at pH 5 which was previously reported to be the optimum pH for the hydrolysis activity of wide-type MalA [30]. However, no obvious transfer product was detected by TLC. By contrast, a clear UV-active spot corresponding to a glycosylated product (**2b**) appeared at pH 7–9, and the intensity of the spot was enhanced at pH 8 and 9 (Fig. 3), implying that the deprotonation of a OH group of **2a** at the more basic pH than pH 7 plays a significant role in the *O*-glycosylation by MalA-D416A.

The initial rate of the reactions determined by HPLC using the isolated transfer product as the standard was the highest at pH 9 (Fig. 4) and 45 °C. The reduction of the rates at pH 10 could be explained by the instability of sugar donor **1**, due to the enhancement of its spontaneous hydrolysis at basic conditions [31]. In order to investigate the possibility of the action of another amino acid residue in the active site as the general base catalyst to activate 7-OH group of the flavonoids, the control reactions using para-nitrophenyl α - and β -D-glucopyranosides as the sugar acceptors were conducted, resulting in no transfer product. Therefore, these results revealed that MalA-D416A is able to transfer glucosyl moiety of the glucosyl intermediate to deprotonated hydroxy groups of aryl compounds [27] and flavonoids at pH 9 without the assistance of general base catalytic residue.

With the aim of investigating the substrate spectrum of MalA-D416A in the synthesis of flavonoid *O*- α -glucosides, another diverse 8 congeners including kaempferol **3a** (belonging to flavonol), hesperetin **4a** (flavanone), naringenin **5a** (flavanone), taxifolin **6a** (flavanonol), (+)-catechin **7a** (flavanol), (-)-epicatechin **8a** (flavanol), daidzein **9a**

(isoflavone) and genistein **10a** (isoflavone) were used as the sugar acceptors. To our surprise, all flavonoids employed in the transglycosylation reacted very well, as only single transfer product from each reaction was detected on TLC plate under UV light (Figure S1). When the reaction mixtures were analyzed by LC-MS, only the peaks corresponding to the glucosides with single glucosyl moiety were detected with no peak relevant to glucosides with more than one glucosyl moiety (data not shown).

2.2. Time course analysis

To determine the optimum reaction time to get maximum yield, transglycosylation reactions using 25 mM donor (**1**) and 20 mM quercetin (**2a**) as the substrates were carried out at different pHs. As expected from the pH profile for transglycosylation activity (Fig. 2), the product formation at pH 9 was the fastest compared to those at other pH, and the maximum yield was 99.7% by HPLC analysis after 2 h reaction (Fig. 5). At pH 8 and 8.5 longer reaction time than that at pH 9 was requested to get the maximum yields (98 and 99% by HPLC analysis, respectively) due to the slow reaction rates. After the maximum yield points, the hydrolysis of the transfer product was observed, leading to slightly decrease in the yield.

2.3. Determination of structures of flavonoid *O*- α -glucosides

Next, glycosylation reactions of flavonoids by MalA-D416A (5 mg) were carried out at pH 9 on a preparative scale using **1** (0.125 mmol) and one of flavonoids **2a-10a** (0.1 mmol in 5 mL). The corresponding transfer products (**2b-10b**) were then purified by flash silica gel chromatography with the isolation yields over 90% (Fig. 6).

Then, 2D (COSY, NOESY, HSQC and HMBC) NMR analyses were carried out to identify the structure of these transfer products (Figure S3, S4). Given the NMR data, all signals for anomeric protons ($H1''$) appeared around 5.3–5.6 ppm as typical doublet peaks, indicating the MalA-D416A synthesized a glycosidic linkage between flavonoid and sugar moieties. Because of the low values of coupling constants $J_{1,2}$ (3.2–4.0 Hz) of $H1''$, the anomeric configurations of all the synthetic linkages were α -anomers. Next, the regioselectivity of MalA-D416A was determined by heteronuclear interactions HMBC. The C7 and H8 of flavonoids coupled with the anomeric proton ($H1''$) and carbon ($C1''$) of glucose moiety, respectively, revealing that MalA-D416A catalyzes highly regioselective glycosylation towards hydroxyl group of flavonoids only at O7. Another evidence of the specific regioselectivity of MalA-D416A comes from the NOESY spectra, as $H1''$ of glucose moiety showed interaction only with H8 of the flavonoids, instead of other proton on the phenolic rings.

2.4. Kinetics of transglycosylation reaction catalyzed by MalA-D416A

To investigate the substrate specificity of MalA-D416A, apparent

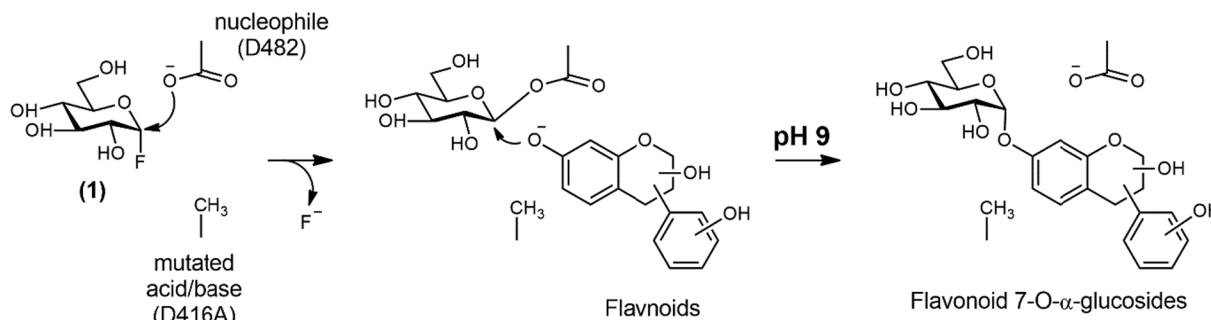


Fig. 2. Scheme of flavonoid *O*- α -glucosides synthesis catalyzed by MalA-D416A using α -D-glucopyranosyl fluoride (**1**) and flavonoids as the sugar donor and acceptors, respectively.

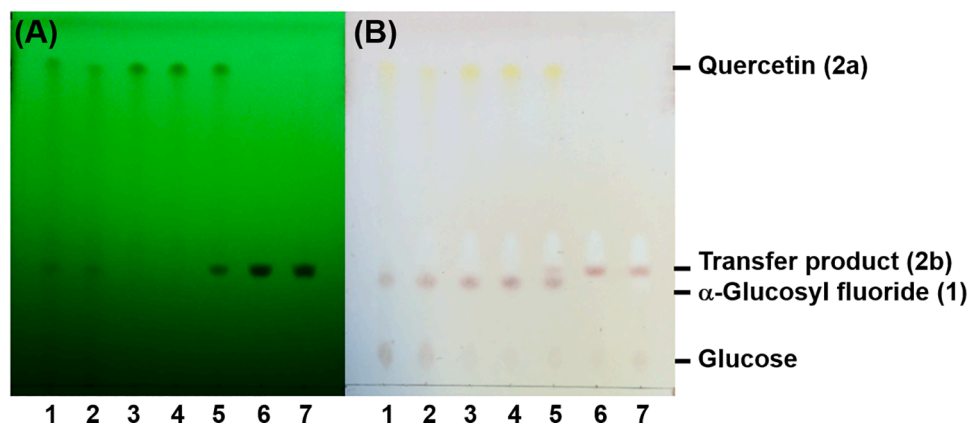


Fig. 3. TLC analysis of transglycosylation reaction using α -glucosyl fluoride (1) and quercetin (2a) as the substrate at different pH. (A) under UV_{254nm}; (B) visualized by H₂SO₄ and charring. Lane 1, 1 and 2a (control); lane 2, 1 and 2a (blank reaction); lane 3, reaction mix at pH 5.0; lane 4, at pH 6.0; lane 5, at pH 7.0; lane 6, at pH 8.0; lane 7, at pH 9.0.

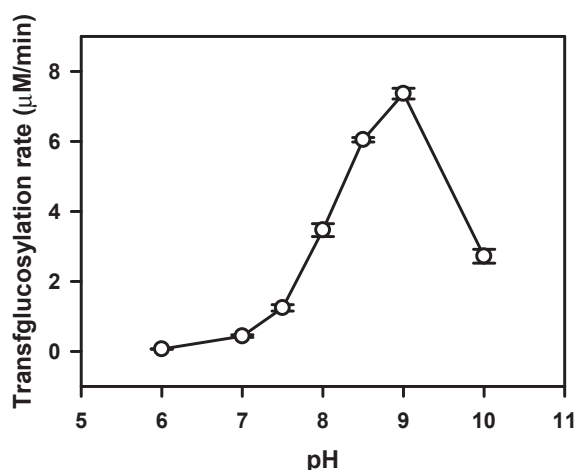


Fig. 4. Effect of pH on transglycosylation activities using α -glucosyl fluoride (1) and quercetin (2a) as the substrates.

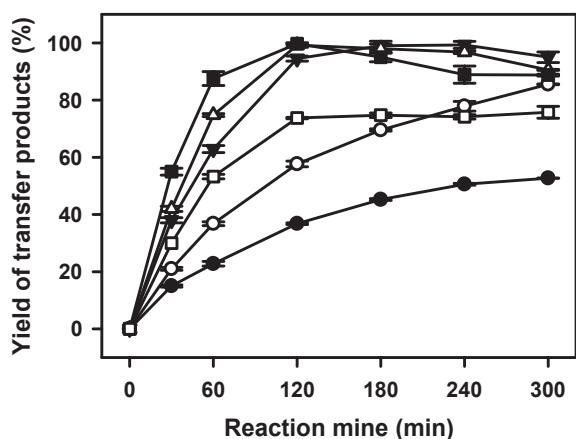


Fig. 5. Time course analysis of the transglycosylation of quercetin (2a) catalyzed by MalA-D416A. Each reaction was conducted at pH 7 (●), pH 7.5 (○), pH 8 (▼), pH 8.5 (△), pH 9 (■), and pH 10 (□).

kinetic parameters were determined at a fixed concentration of either the donor (1) or an acceptor (Table 1 and Figure S2). Given k_{cat}/K_M values for the flavonoids, the flavonoids with the non-aromatic C ring with both oxo group at C4 and hydroxyl group at C5 (4a, 5a, and 6a)

were classified into the good acceptors. The relatively high catalytic efficiency for these acceptors were mainly caused from the higher k_{cat} values than those for 2a and 3a. Of the acceptors, catechins (7a and 8a) lacking the oxo group at C4 and isoflavones (9a and 10a) bearing the B ring at C3 exhibited lower k_{cat}/K_M than the others due to the relatively high K_M values ranging from 0.5 to 1.1 mM. The kinetics analyses revealed that the hydroxyl group at 5-OH and the non-aromatic C ring with the oxo group at C4 give positive effects on the transglycosylation. Upon comparing 6a and 7a, indeed, the only difference is whether the oxo group at C4. In addition, an isoflavone 10a without the OH group at C5 exhibited 2-fold higher K_M value than the other isoflavone 9a. The inappropriate orientation of the ring B in isoflavones would also result in weak affinity toward MalA-D416A. The K_M values for the donor (1) during transglycosylation at a fixed acceptor concentration were lower than that for 4-nitrophenyl α -D-glucopyranoside in hydrolysis by the wild-type MalA enzyme ($K_M = 2.0$ mM) [32], which is consistent with the kinetic reports for acid/base mutants derived from retaining glycosidases [33,34]. Such low K_M of MalA-D416A for the sugar donor 1 implies that flavonoid *O*- α -glycoside synthesis using *O*- α -glycoligases would be more potent than that using glycosynthases with much higher K_M values for fluoride sugars as the donors in the transglycosylation reactions [35].

2.5. *in-silico* modelling of complexes of MalA-D416A and flavonoids

It is worth noting that the transglycosylated products of catechin and epicatechin whose 3'-OH groups on B ring have been proposed as the most acidic OH groups ($pK_{a1} = 8.7$ and 8.9, respectively) [36], also possessed the glucosyl moiety at their 7-OH groups. In addition, the second pK_a values of other flavonoids are around pH 8–9 that would be able to ionize under the basic condition (pH 9), so it could be very likely to generate a mixture of regioisomers. However, MalA-D416A produced only one transfer product, suggesting that the *O*- α -glucosylation by MalA-D416A would be controlled by not only the pH-promoted nucleophilicity of the 7-OH groups of the flavonoids, but also the steric tolerance for the orientation of the 7-OH groups to direct the glucosyl moiety of the glucosyl-enzyme intermediate.

The docking simulations for the model structure of the covalent glucosyl enzyme intermediate with the flavonoids were conducted. The Glide standard precision docking scores of the flavonoids agree with the experimental catalytic efficiencies yielding $R^2 = 0.872$ (Fig. 7A), suggesting that the computational modelling is mostly likely reliable. The complex models exhibited a consistent binding mode for the flavonoids. Given the complex models, it was predicted that the A and C rings of the flavonoids would bind in the subsite + 1 which has been proposed by the crystal structure analysis of the wild type MalA [37]. In addition, the in-

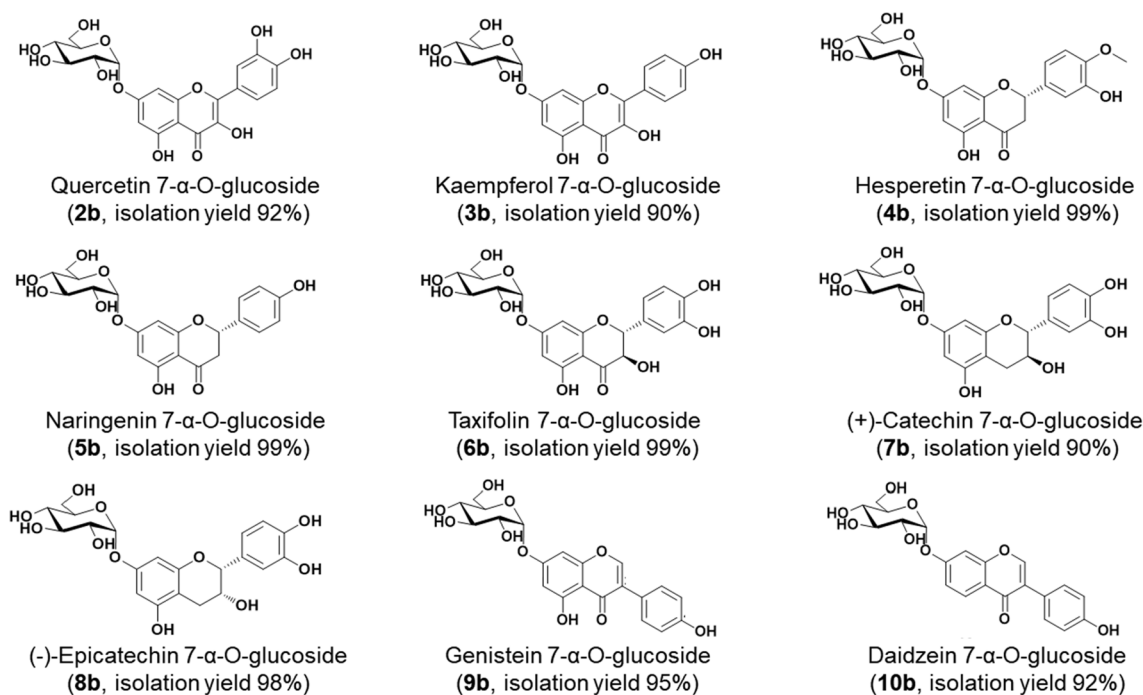


Fig. 6. Structures and isolation yields of flavonoid 7-O- α -glucosides.

Table 1
Kinetic parameters of MalA-D416A.

Substrates		k_{cat} (min ⁻¹)	K_M (mM)	k_{cat}/K_M (min ⁻¹ mM ⁻¹)
varied ^{a)}	fixed ^{b)}			
2a	1	1.3 ± 0.06	0.37 ± 0.04	3.6
3a	1	1.5 ± 0.1	0.34 ± 0.04	4.5
4a	1	2.3 ± 0.1	0.39 ± 0.03	5.8
5a	1	2.5 ± 0.1	0.39 ± 0.04	6.4
6a	1	3.1 ± 0.9	0.25 ± 0.02	12.4
7a	1	1.8 ± 0.1	0.77 ± 0.09	2.4
8a	1	1.6 ± 0.07	0.65 ± 0.08	2.5
9a	1	1.5 ± 0.09	0.52 ± 0.05	2.9
10a	1	1.8 ± 0.1	1.10 ± 0.10	1.6
1	2a	1.4 ± 0.08	0.52 ± 0.05	2.8
1	3a	1.7 ± 0.05	0.49 ± 0.04	3.4
1	4a	2.4 ± 0.1	0.53 ± 0.05	4.6
1	5a	2.6 ± 0.1	0.50 ± 0.04	5.2
1	6a	2.5 ± 0.1	0.53 ± 0.03	6.6
1	7a	1.7 ± 0.08	0.47 ± 0.04	3.5
1	8a	1.5 ± 0.06	0.47 ± 0.03	3.2
1	9a	1.5 ± 0.1	0.53 ± 0.04	2.7
1	10a	1.4 ± 0.1	0.46 ± 0.02	3.1

Reaction condition was 0.2 M Tris-HCl buffer (pH 9.0) at 45 °C.

^{a)} The concentrations were varied up to 2 mM.

^{b)} The concentration was fixed at 2 mM.

silico modelling showed another subsite (subsite + 2) for the binding of ring B, consisting of Y184, A482, T483, D484, and the peptide backbone from F449 to N453 (Fig. 7B). The D87 and D484 of the enzyme would interact with 5-OH and 4'-OH of most of ligands, respectively, through H-bonds (Fig. 7B and 7C). The H-bonding of D87 and D484 with flavonoids and the hydrophobic platform for the binding of the B ring would allow to locate the 7-OH of flavonoids toward glucose moiety of the intermediate, leading to the highly regioselective transglucosylation at 7-OH position. In the case of the isoflavones (9a and 10a), binding of the B-ring in the subsite + 2 would engage in the misorientation of the A and C rings, leading to moving of 7-OH further away from the glucosyl moiety in the intermediate; the distance from the anomeric centre of the glucosyl moiety to 7-OH of 6a and 10a would be 3.3 and 4.6 Å, respectively (Fig. 7C). Indeed, 9a and 10a were one of the poor

acceptors, and the absence of 5-OH in daidzein (10a) made a synergistic negative effect on the catalytic efficiency (Table 1). Unfortunately, these docking complex models did not give clear insight for the role of the oxo group at C4 and non-aromatic C ring for the transglucosylation, which were discussed in section 2.4.

3. Conclusion

The regioselective 7-O- α -glucosylation for flavonoids using an O- α -glycosylase has been successfully accomplished for the first time. Although the detail reaction mechanism of O- α -glucosylation in this study is not fully clear, our findings in this work suggest that the pH-promoted nucleophilicity enhancement of the sugar acceptor at alkaline pH and the steric tolerance of the binding site for flavonoids in the active site of MalA-D416A make it possible to progress the efficient and regioselective O- α -glucosylation for flavonoids. This strategy could be applied to other α -glycosidases to synthesis of various O- α -glucosides derived from phenols, flavonoids, and their analogues. Recently, the synthesis of 1-O-acyl α -L-arabinofuranoses using a thioglycosylase derived from an arabinofuranosidase has been reported [38]. It would therefore be interesting to carry out synthesis of glycosyl esters using O-glycosylases using phenolic acids as acceptors.

4. Materials and methods

4.1. General experiments

MalA-D416A was produced and purified as described previously [24]. Flavonoids and silica gel (200–425 mesh) for flash chromatography were purchased from Sigma-Aldrich. HPLC was carried out with YL9100 HPLC system (Younglin, Anyang, Korea) equipped with a Sun-Fire™ C18 5 μ L column (4.6 \times 150 mm; Waters, Milford, MA). The products were eluted at flow rate 0.8 mL min⁻¹ with acetonitrile/water (30:70, v/v) containing formic acid (0.1%) and analyzed with an ultraviolet (UV) detector under the optimized wavelengths of respective flavonoid product (varied from 220 to 380 nm). ¹H and ¹³C NMR spectra were recorded on a 400 MHz spectrometer (JEOL, Tokyo, Japan) with methanol-*d*₄ as the solvent. Mass data for transfer products were

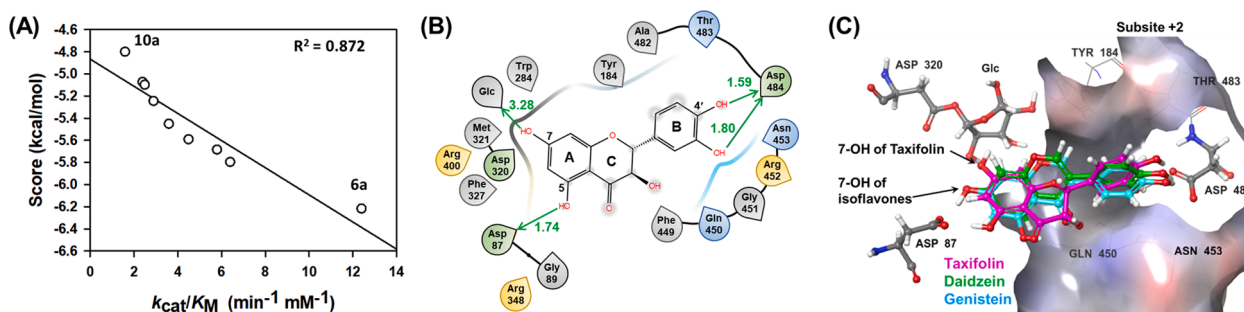


Fig. 7. In-silico modelling for complex structures of the glucosyl enzyme intermediate of MaLA-D416A with flavonoids. (A) Plots of Glide SP scores against experimental catalytic efficiency (k_{cat}/K_M) for nine flavonoids, (B) Interaction between amino acid residues of the glucosyl enzyme intermediate of MaLA-D416A with taxifolin (**6a**). Green arrows and numbers represent H-bonds and their lengths. The residues around **6a** within 4 Å and glucosyl moiety in the intermediate are represented. (C) Superposition of acceptors, **6a**, genistein (**9a**), or daidzein (**10a**) in the complex models of the glucosyl enzyme intermediate. Side chains for the residues are depicted in bond style coloring with carbon atoms in grey. Flavonoids are represented in bond style coloring with carbon atoms in purple (**6a**), cyan (**9a**), or green (**10a**). (For interpretation of the references to colour in this figure legend, the reader is referred to the web version of this article.)

recorded with an LTQ XL linear ion trap mass spectrometer (Thermo Scientific). TLC was performed on aluminum-backed 0.2 mm silica gel 60F₂₅₄ sheets (Whatman/GE Healthcare) with ethyl acetate/methanol/water (17:2:1, v/v/v) containing formic acid (0.1%). The plates were visualized under UV (254 nm) and/or exposure to sulfuric acid (10%) in methanol followed by charring.

4.2. Catalytic properties of MaLA-D416A

The reactions were carried out using 25 mM donor sugar (**1**) and 20 mM quercetin (**2a**) in a buffer (200 mM) containing 30% DMSO and MaLA-D416A (1 mg/mL). To determine optimum pH, the reactions were conducted at a pH ranging from pH 6 to pH 10 and 45 °C. Upon varying temperature, the pH was fixed at pH 9 using 0.2 M Tris-HCl buffer. At each time point the samples were aliquoted and boiled to terminate the reaction. The amount of the glucosyl product (**2b**) was determined by HPLC using a calibration curve which was generated using the purified compound from the preparative scale reaction as the standard. The initial rates of the reactions were determined by linear regression with the data within the 10% consumption of the initial flavonoid. In the case of time course analysis, the reaction was conducted in 200 mM Tris/HCl (pH 9) at 45 °C, and the reaction yield was calculated based on the subjected **2a** as the substrate.

4.3. Preparative scale reaction and structure analysis of transfer products

A mixture of donor sugar (**1**, 0.12 mmol) and acceptor (0.1 mmol) in Tris-HCl buffer (5 mL; 0.2 M; pH 9.0) containing 30% DMSO was treated with MaLA-D416A (1 mg), and the mixture was incubated for 2 h at 45 °C. The flavonoid glucosides were purified on a C18 SEP PAK cartridge (Waters) to remove unreacted sugar, DMSO, proteins and salts. After the solvent was evaporated under reduced pressure, transfer products were isolated by flash silica gel chromatography by solvent gradient elution (ethyl acetate/methanol/water, 17:2:1 to 7:2:1). The structures of purified product were characterized by LC-MS, 1D (¹H and ¹³C) and 2D (COSY, HSQC, HMBC, and NOESY) NMR spectra, successively. The isolation yield of each transfer product was calculated using the weight of the isolated product based on the subjected flavonoid as the substrate.

4.3.1. Quercetin 7- α -O-glucoside (**2b**)

Yellow powder (42.7 mg, isolation yield 92%). ¹H NMR (methanol-*d*₄, 400 MHz): 7.16 (m, 1H, Ph-H2'), 6.92 (m, 1H, Ph-H5'), 6.87 (m, 1H, Ph-H6'), 6.23 (m, 1H, Ph-H6), 5.77 (m, 1H, Ph-H8), 5.52 (d, 1H, *J* = 3.6 Hz, H1'), 3.56 (m, 1H, H4'), 3.50 (m, 1H, H3'), 3.41 (m, 3H, H6' and 2'), 3.32 (m, 1H, H5'). ¹³C NMR (methanol-*d*₄, 100 MHz): 176.47 (C=O); 166.94 (C-7), 158.32 (C-5), 157.74 (C-9), 150.83 (C-4'), 148.25

(C-3'), 147.84 (C2), 137.03 (C3), 122.41 (C-1'), 121.03 (C-6'), 116.96 (C-5'), 116.50 (C-2'), 104.66 (C-10), 97.76 (C-6), 94.40 (C-8) (Ph-C); 101.39 (C-1''), 76.85 (C-3''), 74.42 (C-4''), 73.83 (C-5''), 73.17 (C-2''), 61.87 (C-6''). HMBC shows H1'' coupled with C7 and H8 coupled with C1''. NOESY shows H8 coupled with H1''. ESI-MS: calc. for [C₂₁H₂₀O₁₂ - H⁺]⁻ = 463.4; found 463.4.

4.3.2. Kaempferol 7- α -O-glucoside (**3b**)

Yellow powder (40.4 mg, isolation yield 90%). ¹H NMR (methanol-*d*₄, 400 MHz): 8.05 (m, 2H, Ph-H2' and 6'), 6.83 (m, 2H, Ph-H3' and 5'), 6.68 (m, 1H, Ph-H6), 6.39 (m, 1H, Ph-H8), 5.49 (d, 1H, *J* = 3.2 Hz, H1'), 3.62 (m, 1H, H4''), 3.42 (m, 1H, H3''), 3.36 (m, 3H, H6'' and 2''), 3.18 (m, 1H, H5''). ¹³C NMR (methanol-*d*₄, 100 MHz): 177.70 (C=O); 167.31 (C-7), 159.72 (C-5), 158.29 (C-9), 155.74 (C-4'), 147.37 (C2), 138.31 (C3), 131.98 (2C), 124.04 (C-1'), 117.33 (2C), 105.17 (C-10), 99.92 (C-6), 95.29 (C-8) (Ph-C); 100.03 (C-1''), 76.21 (C-3''), 74.86 (C-4''), 74.16 (C-2''), 73.69 (C-5''), 62.81 (C-6''). HMBC shows H1'' coupled with C7 and H8 coupled with C1''. NOESY shows H8 coupled with H1''. ESI-MS: calc. for [C₂₁H₂₀O₁₁ - H⁺]⁻ = 447.4; found 447.4.

4.3.3. Hesperetin 7- α -O-glucoside (**4b**)

White powder (46.0 mg, isolation yield 99%). ¹H NMR (methanol-*d*₄, 400 MHz): 6.97 (m, 1H, Ph-H2'), 6.82 (m, 2H, Ph-H5' and 6'), 6.36 (m, 1H, Ph-H6), 5.72 (m, 1H, Ph-H8), 5.37 (d, 1H, *J* = 3.6 Hz, H1'), 5.08 (t, 1H, *J* = 4.7 Hz, H2), 3.92 (s, 3H, OCH₃), 3.86 (m, 1H, H4'), 3.67 (m, 1H, H3'), 3.59 (m, 2H, H6''), 3.44 (m, 1H, H2''), 3.31 (m, 2H, H3), 3.19 (m, 1H, H5''). ¹³C NMR (methanol-*d*₄, 100 MHz): 198.50 (C=O); 165.19 (C-7), 162.45 (C-5), 161.99 (C-9), 151.24 (C-4'), 148.17 (C-3'), 132.64 (C-1'), 121.53 (C-6'), 118.95 (C-2'), 116.28 (C-5'), 105.66 (C-10), 98.51 (C-6), 96.46 (C-8) (Ph-C); 97.29 (C-1''), 81.48 (C-2), 76.92 (C-3''), 75.86 (C-4''), 74.68 (C-2''), 73.22 (C-5''), 62.27 (C-6''), 57.24 (OCH₃), 43.52 (C-3). HMBC shows H1'' coupled with C7 and H8 coupled with C1''. NOESY shows H8 coupled with H1''. ESI-MS: calc. for [C₂₂H₂₄O₁₁ - H⁺]⁻ = 463.4; found 463.4.

4.3.4. Naringenin 7- α -O-glucoside (**5b**)

White powder (42.9 mg, isolation yield 99%). ¹H NMR (methanol-*d*₄, 400 MHz): 7.23 (m, 2H, Ph-H2' and 6'), 6.76 (m, 2H, Ph-H3' and 5'), 6.18 (m, 2H, Ph-H6 and 8), 5.47 (d, 1H, *J* = 3.4 Hz, H1'), 5.19 (t, 1H, *J* = 5.5 Hz, H2), 3.71 (m, 1H, H4''), 3.56 (m, 1H, H3''), 3.43 (m, 3H, H6' and 2''), 3.28 (m, 2H, H3), 3.16 (m, 1H, H5''). ¹³C NMR (methanol-*d*₄, 100 MHz): 197.29 (C=O); 168.42 (C-7), 161.86 (C-5), 160.42 (C-9), 154.21 (C-4'), 132.60 (C-1'), 130.65 (2C), 118.37 (2C), 104.28 (C-10), 97.18 (C-6), 95.83 (C-8) (Ph-C); 101.29 (C-1''), 79.63 (C-2), 76.10 (C-4''), 75.89 (C-3''), 74.52 (C-2''), 72.77 (C-5''), 64.13 (C-6''), 42.96 (C-3). HMBC shows H1'' coupled with C7 and H8 coupled with C1''. NOESY shows H8 coupled with H1''. ESI-MS: calc. for [C₂₁H₂₂O₁₀ - H⁺]⁻ =

433.4; found 433.4.

4.3.5. Taxifolin 7- α -O-glucoside (**6b**)

White powder (46.2 mg, isolation yield 99%). ^1H NMR (methanol- d_4 , 400 MHz): 7.01 (m, 1H, Ph-H2'), 6.86 (m, 1H, Ph-H5'), 6.80 (m, 1H, Ph-H6'), 6.39 (m, 1H, Ph-H6), 5.84 (m, 1H, Ph-H8), 5.45 (m, 1H, H2), 5.41 (m, 1H, H3), 5.36 (d, 1H, $J = 3.2$ Hz, H1'), 3.72 (m, 1H, H4'), 3.63 (m, 1H, H3''), 3.55 (m, 2H, H6''), 3.42 (m, 1H, H2''), 3.34 (m, 2H, H3), 3.26 (m, 1H, H5''). ^{13}C NMR (methanol- d_4 , 100 MHz): 197.58 (C=O); 167.29 (C-7), 163.77 (C-5), 162.27 (C-9), 148.86 (C-4'), 147.41 (C-3'), 130.37 (C-1'), 120.65 (C-6'), 116.33 (C-2'), 115.24 (C-5'), 101.48 (C-10), 99.85 (C-6), 97.28 (C-8) (Ph-C); 98.26 (C-1''), 86.53 (C-2), 75.73 (C-3''), 74.51 (C-4''), 74.10 (C-2''), 73.74 (C-5''), 70.81 (C-3), 63.62 (C-6''). HMBC shows H1'' coupled with C7 and H8 coupled with C1''. NOESY shows H8 coupled with H1''. ESI-MS: calc. for $[\text{C}_{21}\text{H}_{22}\text{O}_{12} - \text{H}^+]^- = 465.4$; found 465.4.

4.3.6. (+)-Catechin 7- α -O-glucoside (**7b**)

White powder (40.7 mg, isolation yield 90%). ^1H NMR (methanol- d_4 , 400 MHz): 7.14 (m, 1H, Ph-H2'), 6.95 (m, 1H, Ph-H5'), 6.87 (m, 1H, Ph-H6'), 5.81 (m, 1H, Ph-H6), 5.67 (m, 1H, Ph-H8), 5.48 (d, 1H, $J = 4.0$ Hz, H1''), 5.03 (m, 1H, H2), 4.52 (m, 1H, H3), 3.82 (m, 1H, H4'), 3.64 (m, 1H, H3''), 3.58 (m, 3H, H6'' and 2''), 3.48 (m, 2H, H3), 3.25 (m, 1H, H5''), 2.68 (m, 2H, H4). ^{13}C NMR (methanol- d_4 , 100 MHz): 159.35 (C-7), 158.21 (C-5), 157.83 (C-9), 145.26 (C-4'), 145.87 (C-3'), 130.29 (C-1'), 120.93 (C-6'), 116.39 (C-5'), 115.35 (C-2'), 99.52 (C-10), 94.34 (C-6), 92.64 (C-8) (Ph-C); 99.01 (C-1''), 85.49 (C-2), 77.53 (C-3''), 75.28 (C-4''), 73.96 (C-5''), 73.43 (C-2''), 67.36 (C-3), 62.74 (C-6''), 29.28 (C-4). HMBC shows H1'' coupled with C7 and H8 coupled with C1''. NOESY shows H8 coupled with H1''. ESI-MS: calc. for $[\text{C}_{21}\text{H}_{24}\text{O}_{11} - \text{H}^+]^- = 451.4$; found 451.4.

4.3.7. (-)-Epicatechin 7- α -O-glucoside (**8b**)

White powder (44.3 mg, isolation yield 98%). ^1H NMR (methanol- d_4 , 400 MHz): 7.06 (m, 1H, Ph-H2'), 6.82 (m, 1H, Ph-H5'), 6.73 (m, 1H, Ph-H6'), 5.72 (m, 1H, Ph-H6), 5.60 (m, 1H, Ph-H8), 5.45 (d, 1H, $J = 3.9$ Hz, H1''), 5.01 (m, 1H, H2), 4.46 (m, 1H, H3), 3.78 (m, 1H, H4'), 3.60 (m, 1H, H3''), 3.53 (m, 3H, H6'' and 2''), 3.44 (m, 2H, H3), 3.19 (m, 1H, H5''), 2.62 (m, 2H, H4). ^{13}C NMR (methanol- d_4 , 100 MHz): 158.37 (C-7), 158.02 (C-5), 157.29 (C-9), 144.83 (C-4'), 144.17 (C-3'), 129.66 (C-1'), 119.18 (C-6'), 114.76 (C-5'), 114.23 (C-2'), 98.24 (C-10), 94.39 (C-6), 92.20 (C-8) (Ph-C); 100.16 (C-1''), 85.08 (C-2), 76.36 (C-3''), 76.02 (C-4''), 74.59 (C-5''), 73.29 (C-2''), 66.33 (C-3), 60.22 (C-6''), 26.36 (C-4). HMBC shows H1'' coupled with C7 and H8 coupled with C1''. NOESY shows H8 coupled with H1''. ESI-MS: calc. for $[\text{C}_{21}\text{H}_{24}\text{O}_{11} - \text{H}^+]^- = 451.4$; found 451.4.

4.3.8. Genistein 7- α -O-glucoside (**9b**)

White powder (41.0 mg, isolation yield 95%). ^1H NMR (methanol- d_4 , 400 MHz): 8.12 (s, 1H, C = CH), 7.37 (m, 2H, Ph-H2' and 6'), 6.83 (m, 2H, Ph-H3' and 5'), 6.72 (m, 1H, Ph-H6), 6.58 (m, 1H, Ph-H8), 5.48 (d, 1H, $J = 3.6$ Hz, H1''), 3.52 (m, 1H, H4''), 3.46 (m, 1H, H3''), 3.39 (m, 3H, H6'' and 2''), 3.31 (m, 2H, H3), 3.14 (m, 1H, H5''). ^{13}C NMR (methanol- d_4 , 100 MHz): 180.74 (C=O); 167.21 (C-7), 161.63 (C-5), 157.73 (C-9), 156.23 (C-4'), 153.28 (C2), 132.82 (2C), 125.89 (C3), 124.44 (C-1'), 117.12 (2C), 104.63 (C-10), 97.28 (C-6), 94.51 (C-8) (Ph-C); 100.64 (C-1''), 75.51 (C-3''), 74.68 (C-4''), 74.07 (C-2''), 72.68 (C-5''), 61.33 (C-6''). HMBC shows H1'' coupled with C7 and H8 coupled with C1''. NOESY shows H8 coupled with H1''. ESI-MS: calc. for $[\text{C}_{21}\text{H}_{20}\text{O}_{10} - \text{H}^+]^- = 431.4$; found 431.4.

4.3.9. Daidzein 7- α -O-glucoside (**10b**)

White powder (38.3 mg, isolation yield 92%). ^1H NMR (methanol- d_4 , 400 MHz): 8.28 (s, 1H, C = CH), 8.01 (m, 1H, H5), 7.32 (m, 2H, Ph-H2' and 6'), 7.14 (m, 1H, Ph-H6), 7.03 (m, 1H, Ph-H8), 6.78 (m, 2H, Ph-H3' and 5'), 5.56 (d, 1H, $J = 3.6$ Hz, H1''), 3.63 (m, 1H, H4''), 3.56 (m, 1H,

H3''), 3.45 (m, 3H, H6'' and 2''), 3.37 (m, 2H, H3), 3.24 (m, 1H, H5''). ^{13}C NMR (methanol- d_4 , 100 MHz): 178.26 (C=O); 166.73 (C-7), 158.34 (C-9), 157.59 (C-4'), 153.27 (C2), 130.69 (2C), 129.57 (C-5), 125.49 (C-1'), 123.74 (C3), 118.69 (C-10), 117.73 (2C), 115.48 (C-6), 99.36 (C-8) (Ph-C); 105.83 (C-1''), 76.35 (C-3''), 74.93 (C-4''), 73.74 (C-2''), 72.02 (C-5''), 61.40 (C-6''). HMBC shows H1'' coupled with C7 and H8 coupled with C1''. NOESY shows H8 coupled with H1''. ESI-MS: calc. for $[\text{C}_{21}\text{H}_{20}\text{O}_9 - \text{H}^+]^- = 415.4$; found 415.4.

4.4. Kinetic analysis of transglycosylation catalyzed by MalA-D416A

All kinetic studies were carried out at 45 °C in Tris-HCl (0.2 M, pH 9.0). The amount of released fluoride ion was detected by using a fluoride electrode (Thermo Scientific). The concentration of the donor or acceptor sugar was fixed (2 mM), while that of the counterpart was varied. For fluoride electrode analysis, a standard curve was generated by using various concentrations of fluoride ion solution containing DMSO (30%). All enzymatic rates were corrected for the spontaneous hydrolysis rate of **1**. The apparent K_M and k_{cat} values were determined by fitting the initial velocity curves to the Michaelis-Menten equation by nonlinear regression in GraFit (Erithacus Software, UK).

4.5. Model structure preparation

The flavonoid structures were generated by the 2D Sketcher in Maestro (Schrödinger Release 2019-3, Schrödinger, LLC), after which LigPrep (Schrödinger Release 2019-3) was used to convert them into 3D structures. During the preparation, the force field was set to OPLS3, and all the combinations of stereoisomers were generated. MalA cocrystal complex was downloaded from Protein Data Bank (PDB ID: 2G3M). Downloaded files were prepared with Schrödinger's Protein Preparation Wizard. Restrainted minimization was performed to relax only the added hydrogens using Impact with OPLS3 force field. The skew boat conformation of glucosyl moiety was attached to Asp320, the nucleophilic residue of MalA. And then, mutated Asp416 to Ala and stabilized the structure through energy minimization by Prime (Schrödinger Release 2019-3).

4.6. Molecular docking

Schrödinger's Glide [39] was used to predict poses for a given protein–ligand complex. Glide generated the possible binding modes of ligand–protein complexes and scores them with GlideScore, a mixture of interaction energy and parameter-based penalty functions that roughly represents binding energy. The docking algorithm in Glide utilizes a hierarchical search protocol. In the first stage, 5000 poses for each ligand docking were kept from initial generation for refinement. After the refinement 400 poses were kept for minimization using grids during which a maximum of 100 steps were imposed. Finally, the one pose was scored and ranked after minimizations. Selection of the final ligand pose for Glide is done with GlideScore, which is an extension of an empirically based Chem-Score function of Eldridge et al. [40].

Declaration of Competing Interest

The authors declare no conflict of interest.

Acknowledgements

This work was supported by a Research Fellowship Program funded by Korea University, Republic Korea.

Appendix A. Supplementary material

Supplementary data to this article can be found online at <https://doi.org/10.1016/j.bioorg.2020.104581>.

References

- [1] J.P. Spencer, The impact of flavonoids on memory: physiological and molecular considerations, *Chem. Soc. Rev.* 38 (4) (2009) 1152–1161.
- [2] C.G. Fraga, P.I. Oteiza, Dietary flavonoids: Role of (-)-epicatechin and related procyanidins in cell signaling, *Free Radic. Biol. Med.* 51 (4) (2011) 813–823.
- [3] R.M. van Dam, N. Naidoo, R. Landberg, Dietary flavonoids and the development of type 2 diabetes and cardiovascular diseases: review of recent findings, *Curr. Opin. Lipidol.* 24 (1) (2013) 25–33.
- [4] K. Slámová, J. Kapešová, K. Valentová, “Sweet Flavonoids”: Glycosidase-Catalyzed Modifications, *Int. J. Mol. Sci.* 19 (7) (2018) pii: E2126.
- [5] P.C. Hollman, J.M. van Trijp, M.N. Buysman, M.S. van der Gaag, M.J. Mengelers, J. H. de Vries, M.B. Katan, Relative bioavailability of the antioxidant flavonoid quercetin from various foods in man, *FEBS Lett.* 418 (1–2) (1997) 152–156.
- [6] P.C.H. Hollman, M.N.C.P. Bijlsman, Y. van Gameren, E.P.J. Gnossen, J.H.M. de Vries, M.B. Katan, The sugar moiety is a major determinant of the absorption of dietary flavonoid glycosides in man, *Free Radic. Res.* 31 (6) (1999) 569–573.
- [7] A.J. Day, F.J. Cañada, J.C. Díaz, P.A. Kroon, R. Mclauchlan, C.B. Faulds, G. W. Plumb, M.R. Morgan, G. Williamson, Dietary flavonoid and isoflavone glycosides are hydrolysed by the lactase site of lactase phlorizin hydrolase, *FEBS Lett.* 468 (2–3) (2000) 166–170.
- [8] K. Németh, G.W. Plumb, J.G. Berrin, N. Juge, R. Jacob, H.Y. Naim, G. Williamson, D.M. Swallow, P.A. Kroon, Deglycosylation by small intestinal epithelial cell beta-glycosidases is a critical step in the absorption and metabolism of dietary flavonoid glycosides in humans, *Eur. J. Nutr.* 42 (1) (2003) 29–42.
- [9] J. Xiao, Dietary flavonoid aglycones and their glycosides: Which show better biological significance? *Crit. Rev. Food Sci. Nutr.* 57 (9) (2017) 1874–1905.
- [10] N.C. Veitch, R.J. Grayer, Flavonoids and their glycosides, including anthocyanins, *Nat. Prod. Rep.* 28 (10) (2011) 1626–1695.
- [11] H. Park, J. Kim, K.H. Choi, S. Hwang, S.J. Yang, N.I. Baek, J. Cha, Enzymatic synthesis of piceid glucosides using maltosyltransferase from *Caldicellulosiruptor bescii* DSM 6725, *J. Agr. Food Chem.* 60 (33) (2012) 8183–8189.
- [12] H.J. Woo, H.K. Kang, T.T. Nguyen, G.E. Kim, Y.M. Kim, J.S. Park, D. Kim, J. Cha, Y. H. Moon, S.H. Nam, Y.M. Xia, A. Kimura, Synthesis and characterization of ampelopsin glucosides using dextranase from *Leuconostoc mesenteroides* B-1299CB4: glucosylation enhancing physicochemical properties, *Enzyme Microb. Technol.* 51 (6–7) (2012) 311–318.
- [13] A. Noguchi, M. Inohara-Ochiai, N. Ishibashi, H. Fukami, T. Nakayama, M. Nakao, A novel glucosylation enzyme: molecular cloning, expression, and characterization of *Trichoderma viride* JCM22452 α -amylase and enzymatic synthesis of some flavonoid monoglucosides and oligoglucosides, *J. Agric. Food Chem.* 56 (24) (2008) 12016–12024.
- [14] Y.H. Moon, J.H. Lee, D.Y. Jhon, W.J. Jun, S.S. Kang, J. Sim, H. Choi, J.H. Moon, D. Kim, Synthesis and characterization of novel quercetin- α -D-glucopyranosides using glucanase from *Leuconostoc mesenteroides*, *Enzyme Microb. Technol.* 40 (5) (2007) 1124–1129.
- [15] K. De Winter, G. Dewitte, M.E. Dirks-Hofmeister, S. De Laet, H. Pelantová, V. Křen, T. Desmet, Enzymatic Glycosylation of Phenolic Antioxidants: Phosphorylase-Mediated Synthesis and Characterization, *J. Agric. Food Chem.* 63 (46) (2015) 10131–10139.
- [16] Y. Malbert, S. Pizzut-Serin, S. Massou, E. Cambon, S. Laguerre, P. Monsan, F. Lefoulon, S. Morel, I. André, M. Remaud-Simeon, Extending the structural diversity of α -flavonoid glycosides with engineered glucanases, *ChemCatChem* 6 (8) (2014) 2282–2291.
- [17] B. Cobucci-Ponzano, A. Strazzulli, M. Rossi, M. Moracci, Glycosynthases in Biocatalysis, *Adv. Synth. Catal.* 353 (13) (2011) 2284–2300.
- [18] M.R. Hayes, J. Pietruszka, Synthesis of Glycosides by Glycosynthases, *Molecules* 22 (9) (2017) pii: E1434.
- [19] C. Li, L.X. Wang, Chemoenzymatic Methods for the Synthesis of Glycoproteins, *Chem. Rev.* 118 (17) (2018) 8359–8413.
- [20] M. Yang, G.J. Davies, B.G. Davis, A glycosynthase catalyst for the synthesis of flavonoid glycosides, *Angew. Chem. Int. Ed.* 46 (21) (2007) 3885–3888.
- [21] T. Pozzo, J. Romero-García, M. Fajjes, A. Planas, E. Nordberg Karlsson, Rational design of a thermostable glycoside hydrolase from family 3 introduces β -glucosynthase activity, *Glycobiology* 27 (2) (2017) 165–175.
- [22] M. Jahn, J. Marles, R.A.J. Warren, S.G. Withers, Thioglycosylases: Mutant glycosidases for thioglycoside synthesis *Angew. Chem. Int. Ed.* 42 (3) (2003) 352–354.
- [23] Z. Armstrong, S. Reitingner, T. Kantner, S.G. Withers, Enzymatic thioxyloside synthesis: characterization of thioglycoligase variants identified from a site-saturation mutagenesis library of *Bacillus circulans* xylanase, *ChemBioChem* 11 (4) (2010) 533–538.
- [24] Y.W. Kim, A.L. Lovering, H.M. Chen, T. Kantner, L.P. McIntosh, N.C.J. Strynadka, S.G. Withers, Expanding the thioglycoligase strategy to the synthesis of alpha-linked thioglycosides allows structural investigation of the parent enzyme/substrate complex, *J. Am. Chem. Soc.* 128 (7) (2006) 2202–2203.
- [25] Y.W. Kim, R. Zhang, H. Chen, S.G. Withers, O-glycoligases, a new category of glycoside bond-forming mutant glycosidases, catalyze facile syntheses of isoprimeverosides, *Chem Commun* 46 (46) (2010) 8725–8727.
- [26] C. Li, H.J. Ahn, J.H. Kim, Y.W. Kim, Transglycosylation of engineered cyclodextrin glucanotransferases as O-glycoligases, *Carbohydr. Polym.* 99 (2014) 39–46.
- [27] C. Li, J.H. Kim, Y.W. Kim, α -Thioglycoligase-based synthesis of O-aryl α -glycosides as chromogenic substrates for α -glycosidases, *J. Mol. Catal. B: Enzym.* 87 (2013) 24–29.
- [28] H.J. Ahn, C. Li, H.B. Cho, S. Park, P.S. Chang, Y.W. Kim, Enzymatic synthesis of 3-O- α -maltosyl-L-ascorbate using an engineered cyclodextrin glucanotransferase, *Food Chem.* 169 (2014) 366–371.
- [29] L. Weignerová, P. Marhol, D. Gerstorferová, V. Křen, Preparatory production of quercetin-3- β -D-glucopyranoside using alkali-tolerant thermostable α -L-rhamnosidase from *Aspergillus terreus*, *Bioresour. Technol.* 115 (2012) 222–227.
- [30] K.H. Choi, S. Hwang, J. Cha, Identification and characterization of MaIA in the maltose/maltodextrin operon of *Sulfolobus acidocaldarius* DSM639, *J. Bacteriol.* 195 (2013) 1789–1799.
- [31] M. Jahn, H. Chen, J. Müllegger, J. Marles, R.A.J. Warren, S.G. Withers, Thioglycosynthases: double mutant glycosidases that serve as scaffolds for thioglycoside synthesis, *Chem. Commun. (Camb)* 7 (3) (2004) 274–275.
- [32] M. Rolfmeier, C. Haseltine, E. Bini, A. Clark, P. Blum, Molecular characterization of the α -glucosidase gene (maIA) from the hyperthermophilic archaeon *Sulfolobus solfataricus*, *J. Bacteriol.* 180 (5) (1998) 1287–1295.
- [33] N.O. Tshililo, A. Strazzulli, B. Cobucci-Ponzano, L. Maurelli, R. Iacono, E. Bedini, M.M. Corsaro, E. Strauss, M. M., The α -Thioglycoligase Derived from a GH89 α -N-Acetylglucosaminidase Synthesizes α -N-Acetylglucosamine-Based Glycosides of Biomedical Interest, *Adv. Synth. Catal.* 359(4) (2017) 663 – 676.
- [34] J. Müllegger, M. Jahn, H.M. Chen, R.A.J. Warren, S.G. Withers, Engineering of a thioglycoligase: randomized mutagenesis of the acid-base residue leads to the identification of improved catalysts, *Protein Eng. Des. Sel.* 18 (1) (2005) 33–40.
- [35] Y.W. Kim, S.S. Lee, R.A. Warren, J., S.G. Withers, Directed evolution of a glycosynthase from *Agrobacterium* sp. increases its catalytic activity dramatically and expands its substrate repertoire, *J. Biol. Chem.* 279(41) (2004) 42787–42793.
- [36] J.M. Herrero-Martínez, M. Sanmartín, M. Rosés, E. Bosch, C. Ràfols, Determination of dissociation constants of flavonoids by capillary electrophoresis, *Electrophoresis* 26 (10) (2005) 1886–1895.
- [37] H.A. Ernst, L. Lo Leggio, M. Willemöös, G. Leonard, P. Blum, S. Larsen, Structure of the *Sulfolobus solfataricus* α -Glucosidase: Implications for Domain Conservation and Substrate Recognition in GH31, *J. Mol. Biol.* 358 (4) (2006) 1106–1124.
- [38] Q. Pavic, S. Tranchimand, L. Lemière, L. Gentil, Diversion of a thioglycoligase for the synthesis of 1-O-acyl arabinofuranoses, *Chem. Commun.* 54 (44) (2018) 5550–5553.
- [39] T.A. Halgren, R.B. Murphy, R.A. Friesner, H.S. Beard, L.L. Frye, W.T. Pollard, J. L. Banks, *J. Med. Chem.* 47 (2004) 1750–1759.
- [40] M.D. Eldridge, C.W. Murray, T.R. Auton, G.V. Paolini, R.P. Mee, Empirical scoring functions: 1. The development of a fast empirical scoring function to estimate the binding affinity of ligands in receptor complexes, *J. Comput.-Aided. Mol. Des.* 11 (1997) 425–445.